



Bronze Age vitreous materials from Central Italy: A first insight through an interdisciplinary and multi analytical approach

Silvia Vettori ^{a,*}, Francesca Giannetti ^b, Eleonora Braschi ^c, Riccardo Avanzinelli ^b, Carlo Virili ^d, Alessandro M. Jaia ^d, Alessandro Zanini ^e, Emma Cantisani ^a

^a Institute of Heritage Science, National Research Council of Italy (ISPC – CNR), Italy

^b Earth Sciences Department, University of Florence, Italy

^c Institute of Geosciences and Earth Resources, National Research Council of Italy (IGG – CNR), Italy

^d Department of Classics, Sapienza – University of Rome, Italy

^e Indipendent Archaeologist, ICOMOS Member, Italy

ARTICLE INFO

Keywords:

Vitreous materials
Recent Bronze Age
Central Italy
Non-invasive techniques
p-XRF
SEM-EDS
EMPA

ABSTRACT

An interdisciplinary and multi-analytical approach – combining non-invasive and non-destructive with micro-destructive techniques – has been applied, for the first time, to glass artifacts from Central Italy dating from the Middle Bronze Age to the Early Iron Age. This research provides the unique and extraordinary opportunity to investigate glass materials shedding light on ancient glassmaking techniques and tracing the trade networks that shaped the distribution of these artifacts across Central Italy.

The non-invasive and non-destructive techniques (i.e. p-XRF, FORS and XRD) provided a preliminary characterisation of all the analysed samples that was used to further identify and select a considerably reduced number of artefacts to be investigated by micro destructive ones (i.e. SEM-EDS and EMPA). The combination of all these techniques allowed to identify two main glass types. The majority of the samples display the chemical composition of LMHK glass (one of which High-K) with several characteristics comparable to those from Northern Italian production centres. One sample displays instead a composition typical of natron glasses, with similarities to glass artifacts produced in the Eastern Mediterranean and Egypt. Two main types of chromophores play a role in the origin of the blue colour, Cu and Co. Sb was used to impart both the opacity and the white coloration.

The findings of this work suggests that this archaeological site was included in an international framework of long-distance trade and confirm the importance of the Paduli archaeological site in Central Italy at the end of the II millennium B.C. Here, phenomena of social complexity seem to have emerged with the presence of nascent local elites capable of inserting themselves into the network of international traffic.

1. Introduction

Over the recent decades, the analytical study of ancient glass has allowed an extraordinary advance in the understanding of the ancient world (Henderson, 2013). Chemical, mineralogical and textural analyses together with geochemical and isotopic determinations allow the identification of the different recipes used for ancient glass production, the level of technology reached, the nature and the origin of the raw materials. These analyses can also help to trace the diffusion of the

manufactured objects and/or to locate geographically the primary glass workshop (Angelini et al., 2019). In studies of Italian and European protohistory, the integration of archaeometric data with the traditional study of archaeological materials is a work in progress. Despite the lack of standardised and commonly shared intervention protocols or analytical procedures, this multi-disciplinary approach has proved fundamental for investigating the evolution over time of the different recipes used to produce ancient glass and for tracing the exchange networks between different regional areas.

* Corresponding author at: Institute of Heritage Science, National Research Council of Italy (ISPC – CNR), Via Madonna del Piano 10, 50019 Sesto Fiorentino, Florence, Italy.

E-mail addresses: silvia.vettori@cnr.it (S. Vettori), francesca.giannetti@unifi.it (F. Giannetti), eleonora.braschi@igg.cnr.it (E. Braschi), riccardo.avanzinelli@unifi.it (R. Avanzinelli), carlo.virili@uniroma1.it (C. Virili), alessandro.jaia@uniroma1.it (A.M. Jaia), azanini@azanini.it (A. Zanini), emma.cantisani@cnr.it (E. Cantisani).

In this work, we present the first archaeometric study of Middle Bronze Age (17th – 16th cent. B.C.) to the Early Iron Age (10th cent. B.C.) glass materials from Central Italy (Table 1S in the [Supplementary Materials](#)), specifically from the lakeshore settlement of Paduli (Colli sul Velino, Rieti), performed through a multi-analytical approach that combines non-invasive and non-destructive with micro-destructive techniques.

Several studies have investigated Protohistoric glassy materials from Northern Italy and Sicily (e.g., [Angelini et al., 2002, 2003, 2004, 2005, 2006, 2019; Towle et al., 2001; Arletti et al., 2011; Conte et al., 2015, 2016, 2018, 2019](#)), but no analytical data are present in literature for Central Italy. Our study provides the unique opportunity to compare the characteristics of the finds from Paduli (Colli sul Velino, Rieti) with those of the aforementioned studies, in order to determine the glass composition and to trace the distribution routes of these artifacts in Central Italy. Indeed, the finding of hoards with bronze manufactures and exotic objects, such as ivory artifacts and amber pearls, has suggested that this archaeological site was included in an international framework of long-distance trade ([Licordari and Virili, 2021](#)).

The study was performed in two steps, the first based on non-invasive and non-destructive techniques, the second planned and applied to a specific selection of objects, based on the previous data, which were analysed with micro-destructive techniques. The data acquired by the non-invasive approach are crucial and essential as they allow to gain as much information as possible on a large number of glass artefacts in a rapid, low cost and non-destructive way, significantly reducing the number of objects to be sampled ([Fermo et al., 2016; Micheletti et al., 2020; Yatsuk et al., 2023](#)). This approach was adopted to provide a first detailed characterization of the objects (through Optical Microscopy – OM), colouring agents (by Fibre Optics Reflectance Spectroscopy – FORS in the UV–Vis region), elemental composition (determined by portable X-ray Fluorescence – p-XRF) and crystalline phases in the glass matrix (investigated by X-ray Diffractometry – XRD). It is worth stressing that the investigated set of beads represents all the glassy artefacts found in a large area, equal to 20 ha and corresponding to the maximum extent of the site in the Final Bronze Age. Then, on the basis of the gathered information, it has been possible to select a limited, but representative number of objects to be sampled for detailed analyses of the microstructures and chemical composition (through Scanning Electron Microscopy-Energy Dispersive Spectroscopy – SEM-EDS and Electron Probe Microanalysis – EPMA), with the aim of identifying the raw materials used and establishing their origin and, ideally, the manufacturing site. In this regard, the history of glass acquires great importance.

Glass manufacturing uses raw materials to produce a synthetic product ([Henderson, 2013](#)) such as i) SiO_2 from crushed quartz or sand as a network former, ii) a fluxing agent to lower the melting point of silica, and iii) colorants. The classification of the glass type is based on the chemical elements introduced in the glass batch through the fluxing agent. The first man-made glass artefacts, found in the eastern part of the Mediterranean, date back to the 3rd millennium B.C. ([Oppenheim, 1973; Henderson, 2013](#)), but the occurrence of highly coloured glassy objects only becomes common in Mesopotamian and Egyptian archaeological records from the Middle Bronze Age 1 (16th–15th century BCE) onwards ([Lilyquist et al., 1993; Nicholson, 1993; Shortland, 2000; Freestone, 2006; Shortland and Eremin, 2006; Dardeniz et al., 2022](#)). The 14th century BCE marks the earliest evidence of glass-making in the Syro-Levantine area as well ([Dardeniz et al., 2022](#)). These first glassy materials were usually obtained using quartz pebbles as a silica source and plant ash as a fluxing agent ([Sayre and Smith, 1961; Henderson et al., 2005](#)), and they were commonly known as High Magnesium Glass (HMG). HMG artefacts were widespread during the Bronze Age in the whole Mediterranean ([Santopadre & Verità, 2000](#)).

During the Recent and Final Bronze Age, and particularly between the 12th and 10th centuries B.C., another glass type was produced: in this case, the fluxing agent was probably made using leached plant ash

as source of alkali ([Brill, 1992; Angelini et al., 2004](#)), and the obtained material was described as “mixed alkali glass” or Low Magnesium High Potassium (LMHK) ([Henderson, 1988](#)). This type of glass was only found in Europe ([Henderson, 2013](#)), with a particular abundance of findings in excavations carried out in Frattesina di Rovigo (Italy), a relevant glass-production site ([Biavati and Verità, 1989; Brill, 1992; Angelini et al., 2004; Angelini, 2011](#)). In the context of the network of long-distance trade of this period, Frattesina certainly represents the centre of greatest interest and importance for the whole peninsular Italy ([Bellintani and Angelini, 2020](#)) and beyond. LMHK glasses, likely coming from Frattesina, were found in Switzerland, Germany, France, Ireland, England, Greece, Czechia and Poland ([Venclová et al. 2011; Bellintani 2014; Conte et al. 2019; Purowski et al. 2018](#)). This vast settlement was the central place of a cluster of settlements, located at the mouth of the Po River, in which the processing and (re)distribution of metallurgical and valuable products were concentrated. These exchanges connected Europe to the Aegean and Middle East regions and vice versa, passing through Southern Italy. The time of maximum development of this international network is to be placed at the beginning of the final phase of the Bronze Age.

At the beginning of the 1st millennium B.C., natron glasses started being produced in Egypt ([Schlick-Nolte and Werthmann, 2003; Shortland et al., 2006](#)), indicating that the ashes derived from desert plants were replaced, as fluxing agent, by mineral soda (trona, $\text{Na}_2\text{CO}_3 \cdot \text{NaHCO}_3 \cdot 2\text{H}_2\text{O}$). An alternative source of soda might be the Eastern Anatolian Area in Turkey ([Dardeniz 2015](#)).

This type of glass, widely produced since the 8th century BCE in the Mediterranean and Levantine regions, used calcareous sand as source of silica, and was known as Low Magnesium Glass (LMG). During the Iron Age, this type of material could be found from the Middle East to Italy ([Towle et al., 2001; Towle and Henderson, 2004; Arletti et al., 2011; Conte et al., 2019](#)). This transition between the 2nd and 1st millennium BC is therefore one of the key periods in the further development of glassmaking, with the supplanting of the previous plant-ash technology by natron-based production ([Henderson, 2013; Dardeniz, 2015; Conte et al., 2016, 2019](#)). The latter production, which was already (even though scarcely) in use in Egypt ([Moorey, 1985](#)), became predominant during the Iron Age ([Dardeniz, 2015](#)). Therefore, the present study acquires importance not only because it represents one of the first study on glass samples from Central Italy, but also because it provided a way to further investigate the glass-related production and the trade that characterized the Italian peninsula during that time.

2. Archaeological site of protohistoric age of Paduli (Colli sul Velino, RI)

The Department of Classics at Sapienza University of Rome has been engaged since 2015 in the excavation of the lakeshore settlement of Paduli near Lake Piediluco, located in central Apennine Italy between the intramontane basins of Rieti and Terni ([Fig. 1](#)), at the boundary between inland Lazio and southern Umbria.

The research project aims at reconstructing the diachronic evolution of human adaptation to the lacustrine environment. Such environmental niche conditioned and directed both the settlement patterns and the socio-economic and political articulations of a territorial system consisting of a polycentric network of perilastrine settlements, which were close to each other and with a long continuity of life.

The beginning of the occupation of the site of Paduli seems to have begun in the early stages of the Middle Bronze Age, a moment that marked the genesis of a long historical cycle of occupation of the Piediluco basin ([Virili, 2021](#)) that persisted until the end of the ancient phase of the Early Iron Age.

In the late stage of the Recent Bronze Age (about 1200–1150 cent. B.C.) the settlement continued its development with a prevalence of materials attributable to its most advanced phase, a moment that corresponds to the presence of a domestic structure, resting on a reclamation

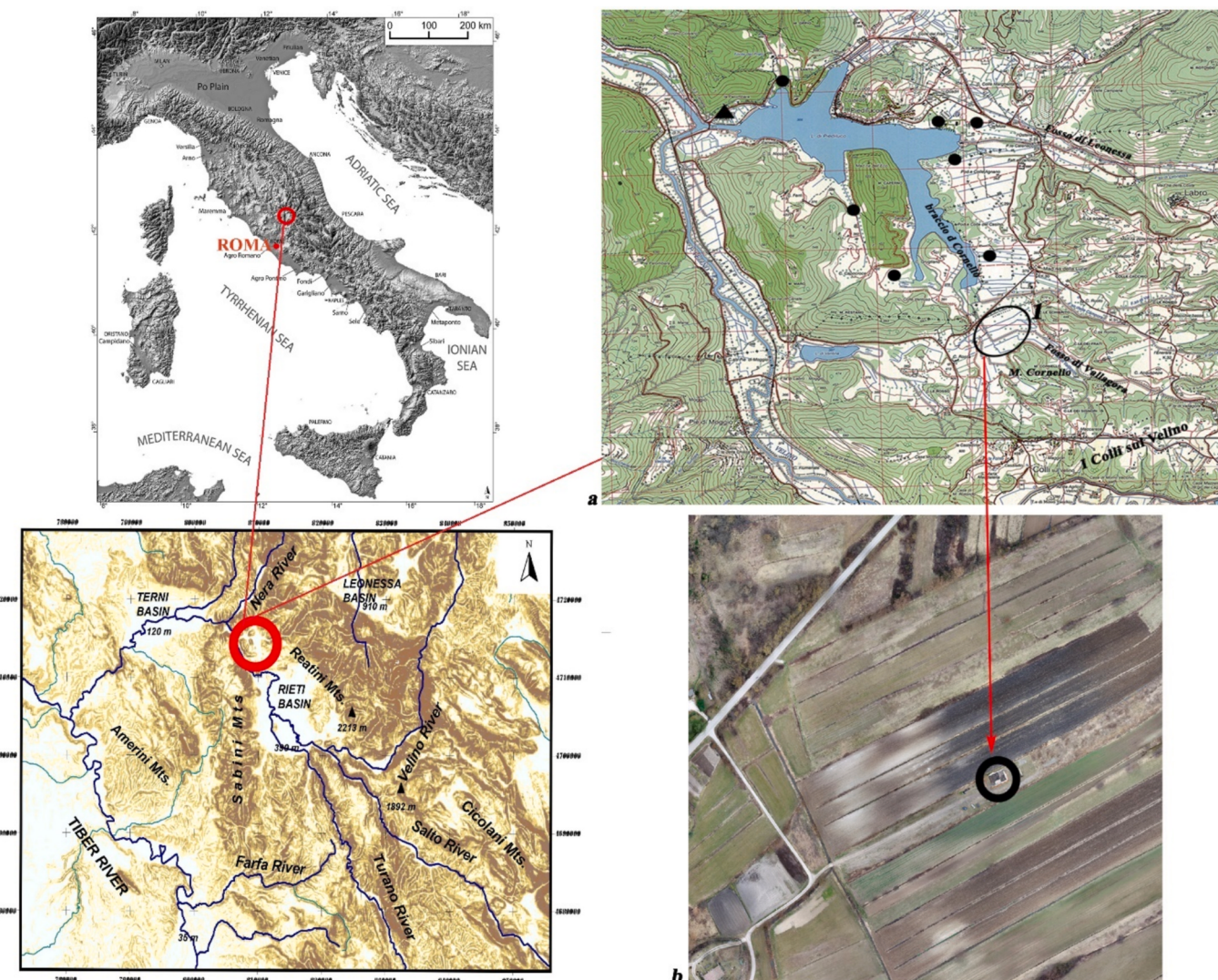


Fig. 1. Study area located in central Apennine Italy, between inland Lazio and southern Umbria (Rieti basin-Terni basin); a) excerpt I.G.M. 1:25,000 (s. 25 DB, 347 IV – Arnone) with distribution of the archaeological sites of the protohistoric age. The dots indicate the settlements; the triangle indicates the area of the Piediluco bronze deposit(s): 1. loc. Paduli (from Virili et al., 2022); b) drone photo of the archaeological site area. The circle indicates the excavation area corresponding to parcel no. 23 (sheet 1 of the municipal register of Colli sul Velino, from Virili et al., 2022).

platform consisting of wooden beams (Jaia et al., 2020).

The Final Bronze Age (about 1150–975 cent. B.C.) represented the period of maximum development of the area, including demographic growth: the Paduli site seems to have occupied, although not continuously, an area of just under 20 ha configuring itself, at the current state of research, as the largest site in the settlement system. Between final phase of the Final Bronze Age and ancient phase of the Early Iron Age (about 975–910 cent. B.C.) the area underwent a transformation in its use, from domestic space to open area. The spaces insisted on walkways made of limestone silt beatings, representing the highest part of an articulated reclamation structure created through successions of material discharges (from which some of the glass materials originated, see Section 3) from previous domestic units. The rubble in turn was cast and levelled over a base platform consisting of a lattice of wooden shingles (Virili, 2022, Fig. 2). This moment possibly brought a mutation of community arrangements, with the emergence of forms of social complexity represented by élites capable of inserting themselves into a network of continental and Mediterranean trades (Baltic amber, Poleian and Aegean glassy materials, ivory, etc.) and of organizing a large-scale metallurgical production with notable Tyrrhenian affinities (Virili et al. 2022).

The local communities had their peak development during the Final Bronze Age and gradually declined during the Iron Age until they disappeared at the beginning of its recent phase perhaps due to the concomitance of a climatic-environmental crisis (rising lake shoreline; Curci et al. forthcoming) and social factors aimed at disrupting the old, partly egalitarian, arrangements (Diamond, 2007). Among the causes of the system's collapse were also historical reasons: the advent of urbanization processes (towards the establishment of larger and more complex agglomerations and territories of relevance) replaced societies based on systems of organized exchange between village communities.

3. Materials and methods

3.1. Vitreous materials

The survey campaigns were preparatory and essential to the excavation activities and have covered, in recent years, an area equal to 20 ha corresponding to the maximum extent of the site in the Final Bronze Age. Most of the vitreous materials of Paduli comes from the survey in the so-called nucleus A, namely (Fig. 3):

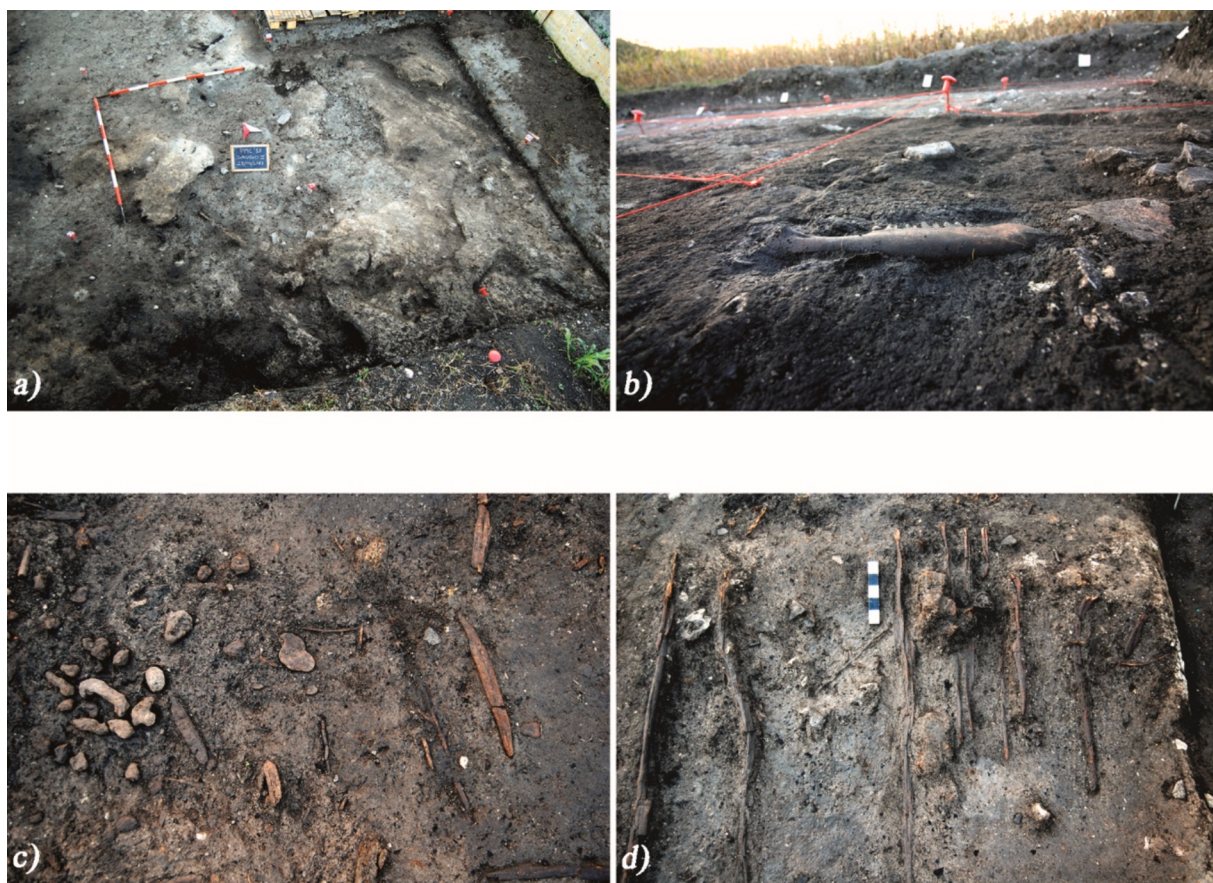


Fig. 2. Walkway system: a) Dig II, calcareous silt floor levels covering the discharges of material; b, c) Dig III, discharges of organic and inorganic materials below floor levels where two vague rings were found (SU 41 and SU 52) and blue barrel-shaped vagus inlaid white spiral thread (SU 52); d) Dig IIII, detail of the arrangement of wooden slats, parallel to each other and equidistant, covered by discharges of organic and inorganic materials.

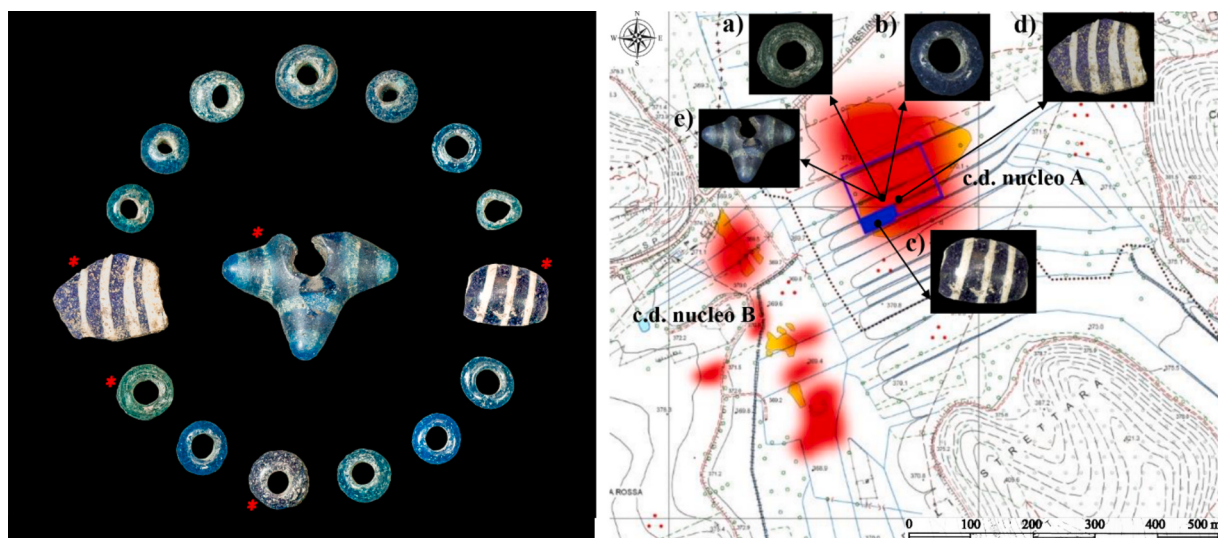


Fig. 3. C.T.R. 1:5,000 (347063 – Madonna della Luce) cross-section of the area in relation to the Paduli archaeological site. The topographic distribution of the glass artefacts (a-b; d-e: from survey; c: from excavation) is presented within the framework of the superficial archaeological deposit. The red patches indicate the areal articulation of the archaeological deposit according to the survey of the Sapienza University of Rome. The boundaries of the area subjected to artefact-level survey are indicated in blue. The area subjected to survey at the artefact level is indicated by the blue rectangle at the corner of the area, which indicates the excavation area. The red asterisks indicate the five artefacts selected for the microsampling.

- 11 beads from blue to turquoise (sample AB_1-11 see [Supplementary Materials Table 2S](#));
- 1 vessel fragment, bichrome blue and white (sample Vf see Table 2S);
- 1 “star” bead with light and dark blue bands (sample STAR see Table 2S).

Three more glass artifacts come instead from the excavation of the filling layers, aimed at raising the floor levels (Fig. 2), dating back between the Final Bronze Age final and the Early Iron Age early (10th cent. B.C.), namely:

- 2 light blue/turquoise beads, very similar to the others (in SU 41 and SU 52; Figs. 2b, c); (sample AB_12-13 see Table 2S);
- 1 blue barrel bead with white spiral decoration (in SU 52; Fig. 2b)¹ (sample BB Table 2S).

Concerning the chronological issue, only these three objects, actually, coming directly from the stratigraphic excavation, can be dated with certainty to the Early Iron Age 1A. For all the other glass artefacts, coming from the survey of the area, therefore, the chronology frame supposed is wide (Table 2S).

3.2. Experimental approach

The multi-analytical protocol for the characterization of ancient glasses was designed and developed at the Institute of Heritage Science of the National Research Council (CNR) in Florence (Italy), in collaboration with the Institute of Geosciences and Earth Resources (CNR) and the Department of Earth Sciences of the University of Florence.

The first step of the analytical protocol involved the use of non-invasive and non-destructive methods, such as p-XRF, FORS, and XRD, carried out directly on glass artefacts as they are. The possibility to carry out a preliminary compositional screening on vitreous materials, allowed us to evaluate the homogeneity in terms of colour, surface characteristics and state of conservation of each sample, and to identify the major and minor elements chromophores elements and the presence of specific crystalline phases.

On the basis of the information gathered in this first step, five representative artefacts were selected for micro-sampling followed by detailed analyses by SEM-EDS and EMPA, for morphological, chromophoric and chemical composition investigation. These are (Fig. 3): i) a light blue/ turquoise annular bead (AB_9); ii) a dark blue annular bead (AB_2); iii) the "star" bead with light and dark blue bands (STAR); iv) a bichrome (blue and white) vessel fragment (Vf); v) a blue barrel bead with white spiral decoration (BB).

3.2.1. Non-invasive and non-destructive techniques

All glass artefacts were examined under a stereomicroscope, model Leica S9i, equipped with a high-resolution camera for photographic acquisitions (see Table 2S).

XRF spectra were collected by means of handheld Tracer III SD Bruker spectrometer, equipped with rhodium anode and solid state silicon detector energy dispersion system. The used set-up was: 40 keV and 12 mA for 120 sec. The measuring area was an elliptical spot of 4 mm × 7 mm.

Spectra were elaborated by PyMCA software.

FORS measurements in the 350–2200 nm range were performed using two single-beam Zeiss spectrum-analyzers, model MC601 (190–1015 nm range) and model MC611 NIR 2.2WR (910–2200 nm range), housed together in a compact and portable chassis for in situ analyses. The data acquisition step was 0.8 nm/pixel for the 1024-element silicon photodiode array detector (MCS601), and 6.0 nm/pixel for the 256-element InGaAs diode array detector (MCS611 NIR 2.2WR). The radiation between 320 nm and 2700 nm, which was provided by a voltage-stabilized 20 W halogen lamp (mod. CLH600), was conveyed to the sample by means of a quartz optical fiber bundle that also transported the reflected radiation to the detectors. Due to the form

and dimension of the samples, spectra were acquired without using a probe head, positioning the fibers end in a way to exclude the specular component of the reflected signal. Each measurement was the average of 3 acquisitions. Calibration was performed by means of a 99 % Spectralon® diffuse reflectance standard. Spectra were processed using Aspect Plus® 1.80 software.

X-ray Diffraction (XRD) data were collected using a Bruker New D8 Da Vinci diffractometer (Cu-K α 1 radiation = 1.54056 Å, 40 kV × 40 mA), equipped with a focussing mirror for incident beam and a Bruker LYNXEYE-XE detector. Samples, as they are, were placed on a Eulerian cradle, allowing the focusing of the X-ray beam on the sample by means of two positioning lasers. Data were collected in the scanning range 20 = 16–62°, with a step size of 0.05° and a counting time of 7 s/step. Phase identification was performed with High Score software.

3.2.2. Micro-destructive techniques

The five selected representative samples were analyzed with a SEM-EDS electronic microscope (ZEISS EVO MA 15) with W filament equipped with analytical system in dispersion of energy EDS/SDD, Oxford Ultimax 40 (40 mm² with resolution 127 eV @5.9 keV) with Aztec 5.0 SP1 software in order to obtain morphological and semi-quantitative analyses. The measurements were performed with the following operative conditions: an acceleration potential of 15 kV, 500 pA beam current, working distance comprised between 9–8.5 mm; 20 s live time as acquisition rate useful to archive at least 600.000 cts, on Co standard, process time 4 for point analyses; 500 μs pixel dwell time for maps acquisition with 1024x768 pixel resolution. The software used for the microanalysis was an Aztec 5.0 SP1 software that employed the XPP matrix correction scheme developed by Pouchou & Pichoir in 1991. This is a Phi-Rho-Z approach which uses exponentials to describe the shape of the φ (pz) curve. XPP matrix correction was chosen because of its favourable performance in situations of severe absorption such as the analysis of light elements in a heavy matrix. The procedure is a "standard-less" quantitative analysis that employs pre-acquired standard materials for calculations. The monitoring of constant analytical conditions (i.e. filament emission) is archived with repeated analyses of a Co metallic standard.

The major elements composition of the samples has been investigated through Electron Microprobe Analysis (EMPA). The quantitative determination of major and selected minor elements (Cu, Sb and Pb), as well as volatiles (Cl and S) was performed using a JEOL Superprobe JXA-8230, equipped with five wavelength-dispersive spectrometers (WDS), under the following operating conditions: 15 kV, beam current at 10nA and beam diameter 10 μm. The peak counting time was of 10 s for Na, 15 s for MgO, Al₂O₃, SiO₂, K₂O, CaO, FeO, TiO₂, 30 s for P₂O₅, Cl, S and 40 s for MnO, Sb₂O₅, PbO, NiO, CoO, ZnO and CuO. The matrix effects were corrected by ZAF algorithm. A selection of natural phases and pure metals is used as primary standard for the elemental calibration (Astimex albite for Si and Na, plagioclase for Al, olivine for Mg, diopside for Ca, sanidine for K, apatite for P, celestine for S, tugtupite for Cl, barite for Ba and Smithsonian ilmenite for Ti and Fe; Astimex pure metal for Pb, Ni, Co, Sb, Zn and Cu). Synthetic reference material glass NIST-SRM1832 and three different Smithsonian Corning glasses (Corning-A NMNH 117218-4, Corning-B NMNH 117218-1 and Corning-D NMNH 117218-3) are used as secondary standards for the analytical quality control. Replicate measurements (10 to 25) on the international reference standards show a good precision with a variation coefficient lower than 1 % for silica, up to 2 % for the other major elements and up to 5 % for minor elements. Accuracy is within 1 % for major and most of minor elements (with the exception of Sb₂O₅ and PbO showing average values within 2 %) and total R² considerably lower than 1 for all the analysed standards.

¹ The vague could fall into the typological category of the so-called pfahlbautönnchenperlen. About the circulation of these artefacts: Jennings 2014; Bellintani 2011, Bellintani & Saracino 2015.

4. Results and discussion

4.1. Non-invasive and non-destructive techniques

4.1.1. Portable X-ray fluorescence spectroscopy

The samples were first analysed by p-XRF to investigate the elemental composition of the glass matrix and to identify the chemical elements responsible for the colouration (Table 1).

The elements detected by p-XRF are Si, S, Cl, K, Ca, Ti, Mn, Fe, Co, Ni, Cu, Zn, As, Sr, Sn, Sb and Pb. We used this technique not to obtain quantitative concentration values, but to provide useful hints about the glass composition. For samples with a silicate glass matrix, only incomplete information can be inferred from p-XRF spectra, and no information can be obtained on important constituents such as, for example, boron, sodium, magnesium, and aluminum oxides ($Z < 14$): therefore, this method cannot provide an accurate estimation of the glass matrix composition (Van der Linden et al., 2011). Light elements are moreover affected by the surface alteration of samples, as the analyzed depth depends on the energy of emitted characteristic X-rays. For this reason, some information on vitreous matrix can be obtained through the comparison of medium Z elements (Fe, Mn and Ti) and the use of Ca to K ratios (Bonizzoni et al., 2013; Micheletti et al., 2020).

The ratio of Ca to K (Table 1) permits to infer the nature of the fluxing agent (Gallo et al., 2013; Van der Linden et al., 2011), in particular distinguishing between three possible fluxing agents employed (i.e. natron, plant and wood ashes). Ca/K ratio higher than 14 is typical of natron, whilst a ratio lower than about 1.5 is interpreted as related to the use of plant ashes (Micheletti et al., 2020). The extreme Ca/K ratio of Vf clearly indicates the use soda (i.e. natron glass) for this sample. All the other samples have lower Ca/K, most of which below 1.5, suggesting the use of plant ashes (i.e., Ca/K < 1.5). Few samples, however, display Ca/K slightly higher than 1.5. These ratios, in fact, permit us to reduce the influence of any systematic error in the determination of elements with comparable energy emissions even if surface alteration still can play an important role, increasing, for example, the considered ratio for a possible loss of K ions (as a consequence of lixiviation).

Mn/Fe and Ti/Fe ratios can provide information about the type of sand used in the glass-making process (Micheletti et al., 2020). In our samples, the Fe/Mn and Fe/Ti remains rather constant in all samples, with a slightly lower ratio only for sample AB_2 (see Table 1), the darker blue bead, showing also the higher Co content. Since Fe and Ti are considered sand impurities – that is oxides naturally associated with sand (Gliozzo et al., 2013) – the data suggest the employment of similar, low iron sands for all the samples and no Mn addition, sometimes used for producing colourless or better manufacturing glass (Micheletti et al.,

Table 1

Ca/K, Mn/Fe, Ti/Fe, Cu/Fe, Co/Fe and Co/Cu ratios obtained for glass samples under investigation. For Co, bdl indicates cobalt content below the detection limit. Ratios are based on net peak areas and elaborated by PyMCA.

Sample	Ca/K	Mn/Fe	Ti/Fe	Cu/Fe	Co/Fe	Co/Cu
AB_1	1.28	0.02	0.18	4.83	bdl	bdl
AB_2	1.71	0.01	0.19	0.78	0.24	0.31
AB_3	2.18	0.02	0.22	8.53	bdl	bdl
AB_4	2.49	0.02	0.22	6.46	bdl	bdl
AB_5	1.13	0.02	0.17	5.29	bdl	bdl
AB_6	0.43	0.02	0.23	8.08	bdl	bdl
AB_7	3.04	0.02	0.33	8.32	bdl	bdl
AB_8	3.60	0.02	0.27	8.75	bdl	bdl
AB_9	1.40	0.04	0.37	6.82	bdl	bdl
AB_10	0.76	0.02	0.29	6.96	bdl	bdl
AB_11	1.44	0.02	0.23	6.30	bdl	bdl
Vf	19.18	0.02	0.11	0.12	0.10	0.86
STAR	1.66	0.02	0.15	5.61	bdl	bdl
AB_12	2.11	0.02	0.31	7.96	bdl	bdl
AB_13	1.16	0.02	0.33	6.42	bdl	bdl
BB	1.07	0.02	0.11	1.12	0.10	0.09

2020).

Blue colouring can be linked to the presence of different metallic oxides, both from the raw (such as Fe) and intentionally added (i.e. Co or Cu) materials. Three darker blue samples (i.e., BB, Vf and AB_2) show higher Co/Fe and Co/Cu than the rest of the samples, which have instead a lighter blue colour. In these three samples some Cu has been also detected, although they show the lowest Cu/Fe among the whole dataset. This suggests that cobalt may contribute, along with copper, to the blue colour of these samples, possibly through mineralisation, such as trianite ($2\text{CoO}_2\cdot\text{CuO}\cdot6\text{H}_2\text{O}$) and skutterudite ($\text{Co}, \text{Fe}, \text{Ni}\text{As}_3$) (Henderson, 1985). The presence of some trace elements such as Ni and As in BB and AB_2 and Pb in Vf may be associated with cobalt-bearing raw material, as observed by Gratuze et al. (1992).

On the other hand, the light blue samples are characterized by high Cu/Fe (>5 , Table 1) and cobalt content under the detection limit, suggesting that copper is the only element responsible for the blue colour.

Moreover, p-XRF data highlight the presence of Sb in the white opaque decorations of the vessel fragment.

4.1.2. Fiber optic reflectance spectroscopy

The use of FORS in the UV–Vis region can provide information on the nature of the chromophore system in a simple way, including the oxidation state of the species responsible for light absorption. Cobalt, for example, is well-known as a metal responsible for deep blue colorations; it has a very high colouring power and can be seen in FORS spectra due to three characteristic absorption bands (540–600–640 nm), more easily than with XRF, where Co $\text{K}\alpha$ emission may be hidden by Fe $\text{K}\beta$ line.

The light blue bulk of the beads mostly produced similar spectra. Representative spectra from the whole sample set are reported in Fig. 4. Most of the samples exhibit spectra similar to that reported for the AB_9 (red spectrum) showing only the presence of Cu^{2+} (broad band centered at about 835 nm) to obtain turquoise/light blue glass (Mirti et al., 2000; Meulebroeck et al., 2010). The strong broadening up to about 1400 nm could suggest also the presence of Fe^{2+} , with its typical broad band that starts to increase at about 1000 nm (Möncke et al., 2014; Meulebroeck et al., 2016), that might contribute to the light blue shades (Micheletti et al., 2020).

The three darker blue samples described in the previous section (i.e. AB_2, Vf and BB) show the presence of the pronounced set of Co^{2+} triple bands at approximately 540, 600 and 640 nm (Mirti et al., 2000; Meulebroeck et al., 2010; Möncke et al., 2014; Meulebroeck et al., 2016) in addition to Cu^{2+} (green spectrum in Fig. 4, related to Vf), consistently with what observed by p-XRF.

4.1.3. X-ray diffraction

XRD patterns were acquired on the whole objects, directly on the bead surface without any preparation in a non-invasive and non-destructive mode and proved the presence of crystalline phases dispersed in the glass matrix, which are responsible for the opacity of the blue and white glass. For many samples the patterns did not show diffraction peaks, suggesting that the number of particles dispersed in the samples is too low to be detected. For few samples, however, the X-ray diffraction revealed peaks that could be used to identify specific mineral phases that may have played a role in the opacity of the glass.

The opacity of the white in the Vf sample is due to the presence of dispersed particles of calcium antimonate as hexagonal CaSb_2O_6 (Fig. 5), a neo-formation phase produced by adding Sb (probably as oxide) to a Ca-rich glass batch or raw glass (Shortland, 2002; Arletti et al., 2006a, 2006b). Experimental studies on the synthesis of pure crystals of Ca antimonate (Butler et al., 1950; Lahil et al., 2008) show that CaSb_2O_6 crystallizes from 927 °C at the expense of $\text{Ca}_2\text{Sb}_2\text{O}_7$ (orthorhombic phase that forms at lower temperatures), and becomes the only phase above 1094 °C. Moreover, a more recent experimental study by Lahil et al. (2010) on syntheses of in situ opacified glass, highlights that both time of fire and temperature play an important role in the crystallization of the two different Ca antimonates phases. The

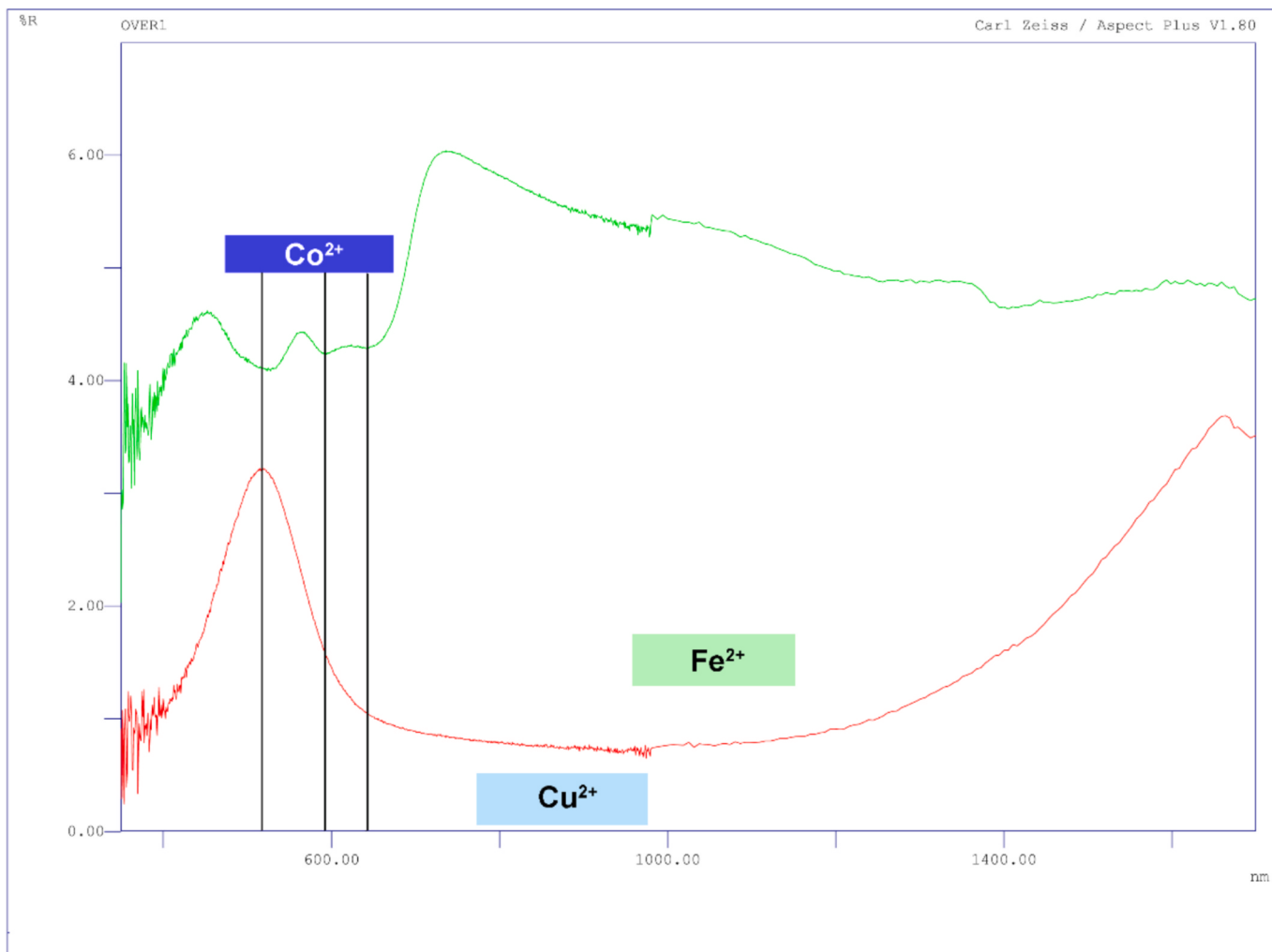


Fig. 4. Representative FORS spectra for the dark blue (in green) and lighter blue (in red) beads, with indicated the characteristic bands (Co^{2+} bands: black vertical lines, Cu^{2+} – light blue area, Fe^{2+} – light green area).

presence of only the hexagonal phase in our sample allows us to hypothesize a high melting temperature for the production of this glass and/or short firing time.

Few other samples reveal the presence of quartz and more often of tridymite. The abundance of the latter mineralogical phase indicates that relatively high temperatures and/or prolonged heating times were used during processing (Artioli et al., 2008). In the AB_9 sample cristobalite has been identified and its presence is important since it is one of the high temperature polymorphs of silica. Pure quartz starts converting into cristobalite above 1300 °C, depending on the heating path and the kinetics, with fast transformation rates above 1470 °C (Stevens et al., 1997). Such high temperature seems too high for the technology of the studied period (e.g., Turner 1954; Henderson, 2013 and reference therein). However, it has been shown that both cristobalite and tridymite are stabilized by the presence of alkali ions, namely Na and K, hence allowing lower temperatures. In fact, Stevens et al. (1997) demonstrate that tridymite does not form at all in alkali-free environments.

4.2. Micro-destructive techniques

As mentioned in Section 3.2 five representative samples were selected on the basis of their shape, colour and compositional characteristics determined through the non-invasive and non-destructive approach. In particular, among the 13 annular beads, we selected: a)

AB_9 has a light blue/turquoise colour (Fig. 3) and several similarities with the other beads, and b) AB_2 that has the darkest colour and the highest Co/Fe ratio. Also the two bichrome blue and white objects (i.e. Vf and BB) and the STAR were selected.

4.2.1. SEM-EDS

Morphological and compositional differences among the selected samples were obtained using a SEM equipped with EDS. Differences in texture homogeneity and in the amount, shape and composition of inclusions were also investigated.

Concerning the two annular beads, sample AB_9 (Fig. 6a), which is the most transparent, presents a homogeneous glass matrix, characterized only by the presence of a few bubbles and an inclusion; sample AB_2 presents, instead, greater inhomogeneity due to the presence of several bubbles and irregularly shaped, spherical inclusions containing elements with higher atomic numbers (lighter colors in BSE, Fig. 6b). Non-reacted inclusion grains are also present, and they are essentially composed of pure SiO_2 . Metallic inclusions are often found, sometimes with a nearly pure copper (Cu) composition (in light blue sample AB_9), other times with copper (Cu) and sulphur (S), and enriched in other metals, most frequently nickel (Ni), cobalt (Co) and arsenic (As) (in dark blue sample AB_2; Fig. 6b).

The Vf sample shows visible morphological and compositional inhomogeneities attributable to the bichromy of the glass material (Fig. 6c). In particular, the areas of white glass appear lighter in the BSE

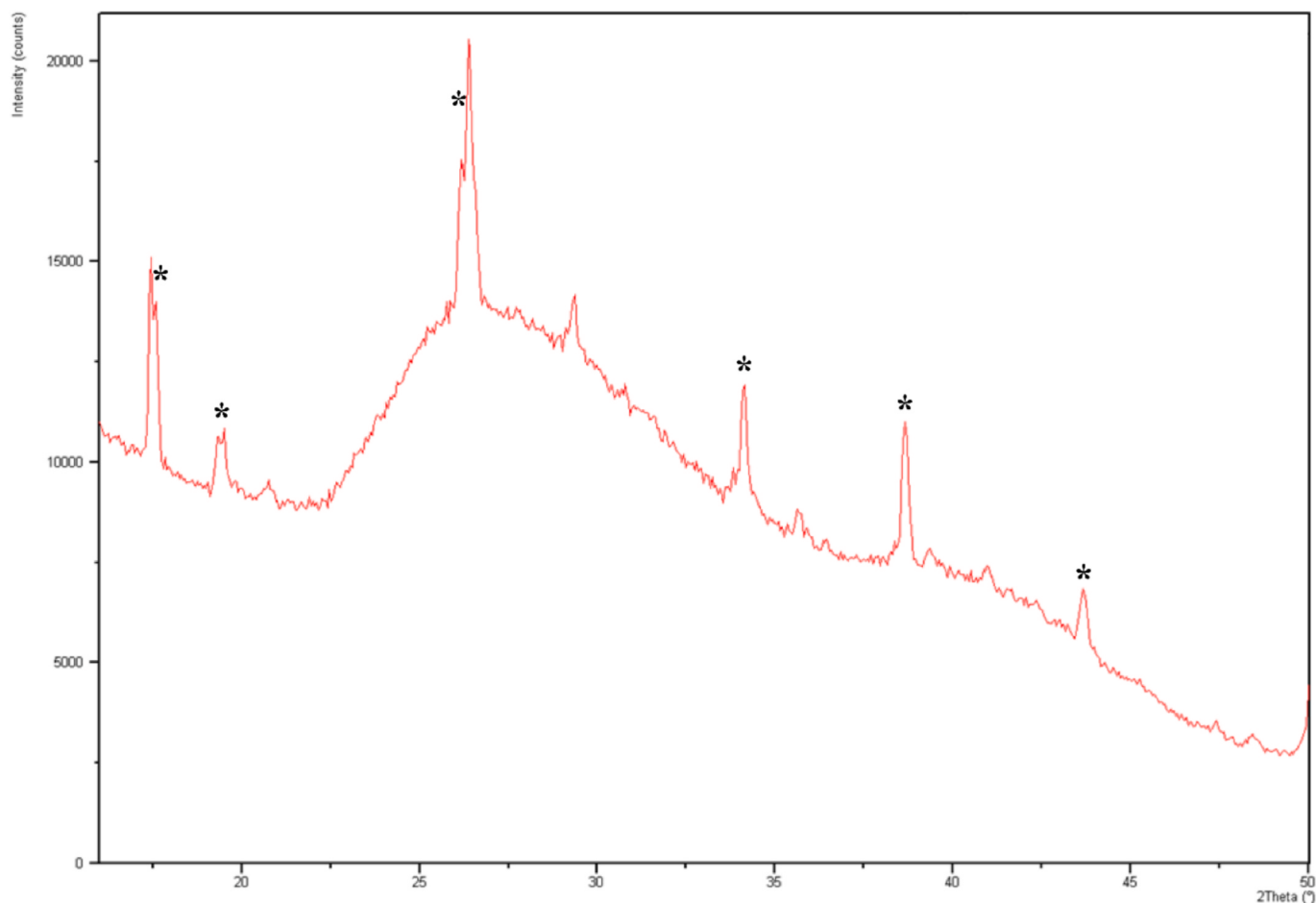


Fig. 5. XRD pattern obtained from surface analysis of the white part of the vessel fragment. The main peaks of calcium antimonate as hexagonal CaSb_2O_6 is evidenced (*).

image, being richer in elements with high atomic number, and are characterized by grains and inclusions of different and irregular shapes. The inclusions present in the white zone, of irregular shape, are finely dispersed in the glass matrix, and they contain calcium (Ca) and antimony (Sb), most probably ascribable to calcium antimoniate compounds, as previously detected by XRD analysis (Fig. 6d). In the blue glass portion, instead, the glass matrix is darker and more homogeneous, but also characterized by the presence of several bubbles and some rounded or sub-rounded grains mainly of SiO_2 and some inclusions. The latter are composed of either cobalt (Co) and iron (Fe), or iron (Fe), antimony (Sb) and lead (Pb).

The BB sample with white spiral decoration has the greatest textural inhomogeneity, not only due to the different composition of the blue and white areas of the glass material, but also for the presence of micro-cracks and many differently shaped grains, sometimes grouped in large rounded or sub-rounded aggregates, and inclusions. The inclusions in the blue zone are composed mostly of copper (Cu), nickel (Ni) and arsenic (As). The white area, instead, shows the presence of grains finely dispersed in the glass matrix containing silicon (Si) and calcium (Ca) (Fig. 6e).

Lastly, the STAR sample, with light and dark blue bands macroscopically visible to the naked eye, is characterized by morphological and textural differences in correspondence of the different bands: the darker blue portion has a more homogeneous texture and is less rich in bubbles (Fig. 6f), whereas the lighter part is richer in acicular SiO_2 inclusions, often present as *glomeruli*. The inclusions containing copper (Cu) are present in both bands.

4.2.2. EMPA

EMP analyses have been performed on the same five samples investigated with SEM-EDS. The data are showed in Table 2 and report, for each sample, the average of several data points (4–13, depending on sample homogeneity) with the associated standard deviation (1 s.d.). For samples with colour variations (i.e. Vf and BB), we report separately the chemical composition of the white (“-W) and blue portion (“-BLUE”). Concerning STAR sample, the distinction has been made taking into consideration the lighter-blue parts and darker-blue parts.

EMPA results will be first used for the glass classification and then discussed grouping the elements according to their affinity to the different components used in the glass making process, as defined by Degryse and Shortland (2020), namely: i) elements related to the type of fluxing agent (i.e., Na, K, Mg, P, Cl, S); ii) element related to the glass stabilizers (i.e., Ca, Mg); iii) network forming elements, linked to the sand (i.e., Si, Al, Fe, Ti, Cr); iv) elements used as glass colourants and associated elements (i.e., Co, Cu, Mn, Sb, Pb, Zn, Ni).

4.2.2.1. Glass classification. The classification of ancient glass generally is based on MgO and K_2O contents (Sayre & Smith, 1961; Henderson, 1988, 1989, Fig. 7a) that are mainly introduced with the fluxing agent.

Fig. 7a shows that Vf pertains to the natron group (characterized by K_2O and $\text{MgO} < 1.5 \text{ wt\%}$) whilst the other four samples (i.e. AB_2, AB_9, BB and STAR both parts) lie within the LMHK field (with $\text{MgO} < 1.5 \text{ wt\%}$ and $\text{K}_2\text{O} > 1.5 \text{ wt\%}$); among these, AB_9 sample can be further classified as a HIGH-K glass (Fig. 7b), having relatively high K_2O content ($> 12 \text{ wt\%}$) together with low Na_2O concentration (1.56 wt\%), distinguishing it from the other LMHK samples discussed in this study (see Conte et al.,

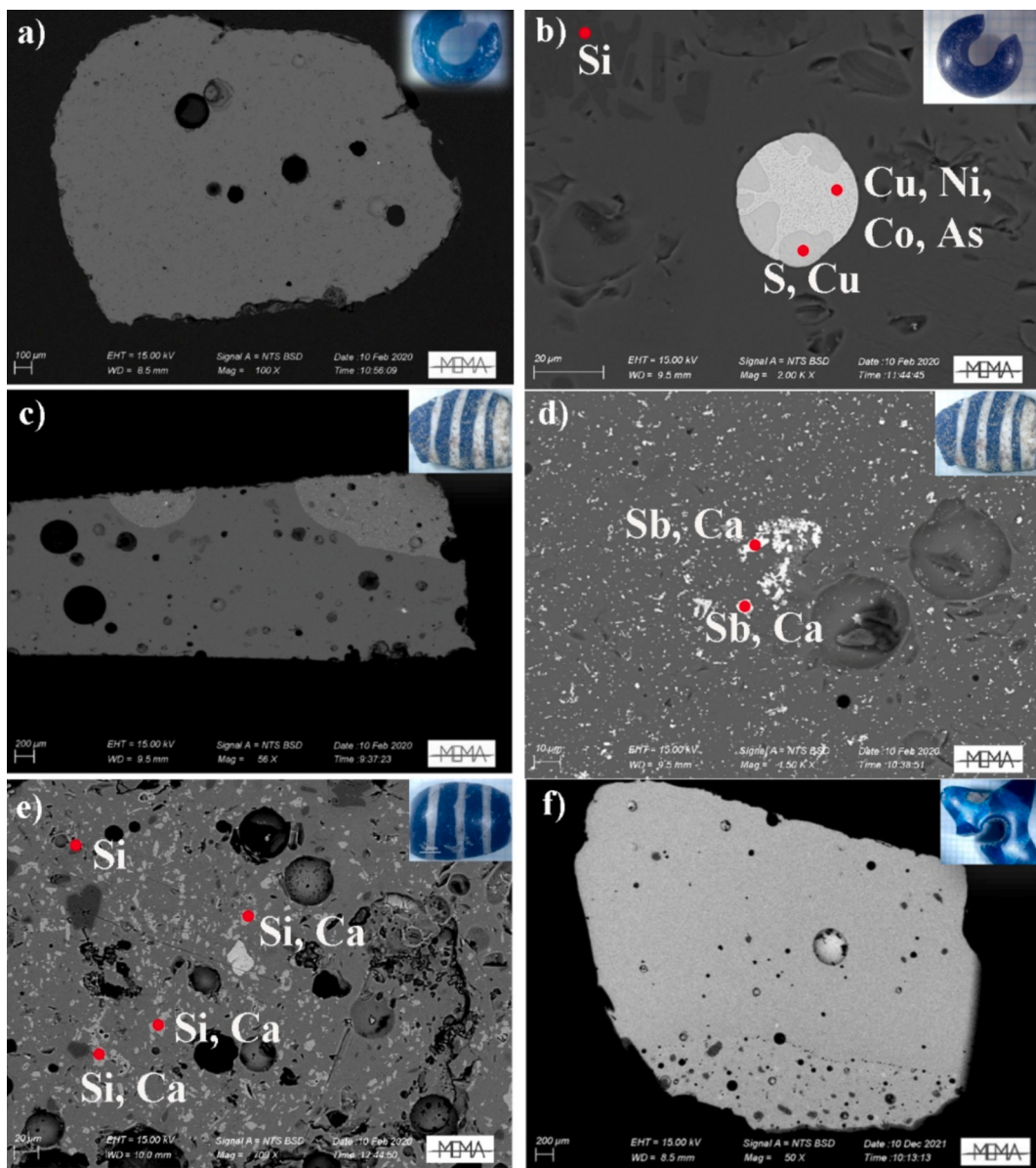


Fig. 6. SEM backscattered electron (BSE) images of a) AB_9 annular bead; b) round-shaped droplet in AB 2 annular bead; c) Vf vessel fragment; d) inclusions containing Ca and Sb dispersed in the glass matrix of the white decoration of Vf; e) grains finely dispersed in the glass matrix containing Si and Ca in the white decoration of BB; f) textural differences of the lighter and darker blue bands in the STAR.

2019; Mildner et al., 2014; 2015).

To integrate and implement this classification we used the Ca/K ratios, previously mentioned as an index of the fluxing agent (Gallo et al., 2013; Van der Linden, 2011; section 4.1.1.), plotted vs the MgO content (Fig. 7c). The figure confirms the use of natron ($\text{Ca}/\text{K} > 14$) only for sample Vf, and of leached ashed plants for all the other samples, in agreement with the evidence deriving from non-invasive and non-destructive methods (i.e. Portable X-ray fluorescence spectroscopy: section 4.1.1).

4.2.2.2. Elements linked to the type of fluxing agent. The Vf sample is characterized by high contents of Na_2O (15.0 ± 0.4 wt% for the blue body and 12.2 ± 0.2 wt% for the white decoration; Table 2) and is also the most enriched in Cl and S, among all the analysed glass samples, confirming the use of soda as fluxing agent and its evaporitic nature, as typically suggested for natron glasses (e.g., Shortland et al., 2006). This is also consistent with the low P_2O_5 content of this samples compared to LMHK ones.

Among the LMHK samples, the HIGH-K AB_9 has the highest K_2O and lowest Na_2O contents, whereas all other samples present comparable Na_2O and K_2O contents. The most accredited hypothesis considers that the fluxing agent of LMHK glasses is produced by the recrystallization of the water used to leach ashes of plants, (Brill, 1992; Hartmann et al., 1997). In this context, the alkali variation among LMHK (including the HIGH-K) samples might be associated with differences in the mixed-alkali technology used in glass making centres (Towle and Henderson, 2004). Different plants, different environments in which these plants grow, and different incineration methods can, indeed, produce fluxing agents with variable proportions of alkali metals (Barkoudah & Henderson, 2006, Towle and Henderson, 2004).

4.2.2.3. Elements linked to the stabilizing agent (Ca, Mg). All samples show higher CaO contents compared to MgO ; therefore, CaO acts as the primary stabilizer in all the samples analysed in this study. Samples with the highest lime (CaO) contents are the AB_9, the BB-W and both Vf-W and BLUE portions. As previously stated (Section 1), the stabilizer in

Table 2

Mean chemical compositions and standard deviations of the 5 samples analyzed by EMPA. Major and minor elements expressed as weight % (element oxide).

ID Sample	AB_9		AB_2		BB-BLUE		BB-W		Vf-BLUE		Vf-W		STAR lighter blue		STAR darker blue	
No. of point analyses	7		9		8		4		5		3		13		8	
	Average	1 s. d.	Average	1 s. d.	Average	1 s. d.										
SiO ₂	73.2	0.5	78.2	0.6	76.2	0.4	74.0	0.5	69.5	0.2	68.0	0.2	75.0	0.4	75.7	0.4
TiO ₂	0.04	0.03	0.06	0.02	0.10	0.02	0.16	0.01	0.06	0.01	0.01	0.01	0.07	0.02	0.07	0.02
Al ₂ O ₃	1.09	0.04	2.38	0.08	2.44	0.02	2.96	0.06	2.45	0.05	2.34	0.06	1.94	0.04	2.01	0.03
Cr ₂ O ₃	bdl	—	bdl	—	0.01	0.01	0.01	0.01	0.01	0.01	0.01	0.02	0.01	0.01	0.01	0.01
FeO	0.39	0.04	0.73	0.09	1.02	0.05	0.97	0.03	0.86	0.04	0.32	—	0.59	0.05	0.45	0.04
MnO	0.01	0.01	0.02	0.01	0.02	0.01	0.02	0.01	0.02	0.01	0.01	0.01	0.02	0.01	0.01	0.01
NiO	bdl	—	0.31	0.14	0.37	0.03	0.02	0.02	0.01	0.01	0.01	0.01	bdl	—	bdl	—
ZnO	bdl	—	0.02	0.02	bdl	—	bdl	—	bdl	—	bdl	—	0.01	0.01	0.02	0.02
MgO	0.61	0.02	0.71	0.03	0.93	0.01	1.35	0.08	0.54	0.02	0.51	0.03	0.80	0.03	0.55	0.03
CaO	6.98	0.17	1.64	0.09	2.33	0.05	6.99	0.25	7.77	0.14	7.01	0.10	1.56	0.04	1.43	0.05
Na ₂ O	1.56	0.03	7.23	0.16	6.47	0.20	6.46	0.19	15.04	0.39	12.17	0.17	7.96	0.26	5.73	0.22
K ₂ O	12.97	0.15	7.90	0.11	7.98	0.21	6.30	0.11	0.39	0.03	0.42	0.03	7.99	0.14	10.27	0.17
P ₂ O ₅	0.28	0.05	0.08	0.08	0.19	0.04	0.19	0.05	0.04	0.03	0.04	0.04	0.18	0.09	0.14	0.08
Sb ₂ O ₅	bdl	—	bdl	—	0.75	0.05	0.33	0.02	0.90	0.06	7.55	0.46	bdl	—	bdl	—
SO ₃	0.04	0.02	0.04	0.02	0.02	0.01	0.02	0.02	0.32	0.02	0.21	0.04	0.04	0.02	0.03	0.01
CuO	3.19	0.46	0.32	0.15	0.97	0.05	0.17	0.03	0.15	0.01	0.01	0.01	2.58	0.07	3.17	0.06
PbO	bdl	—	bdl	—	bdl	—	0.02	0.01	0.20	0.02	0.05	0.02	bdl	—	bdl	—
CoO	bdl	—	0.20	0.01	0.10	0.05	bdl	—	0.16	0.02	0.02	—	bdl	0.01	0.01	0.02
Cl	0.03	0.01	0.17	0.02	0.06	0.02	0.26	0.01	1.14	0.02	1.20	0.17	0.49	0.04	0.10	0.01
Total	100.4	—	99.9	—	100.0	—	100.2	—	99.3	—	99.5	—	99.2	—	99.7	—

*bdl = below detection limit.

plant ash glasses was introduced in the batch together with the fluxing agent (Barkoudah and Henderson, 2006). The fluxing agent of LMHK glasses has been suggested to be somewhat depleted in Ca with respect to plant ash (Hartmann et al., 1997), but it is not known to what extent. Therefore, it is difficult to assess whether Ca in our LMHK samples was introduced together with the fluxing agent or added from other sources.

On the other hand, natron fluxing agent, as that used for Vf-W and BLUE, does not introduce Ca, implying that the stabilizer come from a purposely added component (e.g., marine shells) or from impurities in the silica source (Wedepohl & Baumann, 2000; Freestone et al., 2003, Freestone, 2006). Previous studies (e.g., Freestone et al., 2003) suggest that the CaO content in glasses made from “impure” sand (i.e., with > 3 wt% of Al₂O₃) should be about 1.5 wt%, even assuming that the alumina content was to be totally ascribed to a Ca-rich feldspathic source (i.e., anorthitic feldspar: CaAl₂Si₂O₈). Considering the high CaO content of Vf (>7 wt% in both the white and blue portions) we argue for the introduction of Ca, either added specifically or due to the use of carbonate-rich sands (e.g., costal sands, as in Freestone et al., 2003).

4.2.2.4. Network formers elements, linked to the sand (i.e., Si, Al, Fe, Ti, Cr). As reported in the literature (Henderson et al., 2004; Gliozzo, 2017), Al₂O₃ content < 1 wt% in glass artefacts is linked to the use of a mineralogically mature sand made almost entirely of quartz, whilst Al₂O₃ > 1.5 wt% points to the use of impure silica source, where aluminium is linked to the presence of feldspar or clay minerals together with quartz in the sand. Among our samples, only AB_9 (HIGH-K) displays such a low Al₂O₃ concentration (1.09 wt%). All the other ones have Al₂O₃ contents ranging from 1.94 to 2.96 wt%, hence arguing against the use of a mineralogically mature sand. On the other hand, all the analysed samples display relatively low FeO, TiO₂ and Cr₂O₃ concentrations, which may also identify other possible impurities. Overall, the EMPA data points to the use of a sand made of quartz and only minor amount of feldspar (relatively rich in Al, but devoid of Fe, Ti and Cr), possibly containing also carbonates as discussed above.

4.2.2.5. Elements used as glass colourants and associated elements (i.e., Co, Cu, Mn, Sb, Pb, Ni). EMPA data confirm the evidence provided by non-invasive and non-destructive methods, indicating that the blue colour of the beads (therefore not considering the white decorations of

the BB and Vf) is to be associated with the relatively high contents of Cu and Co. The samples with the lightest colour (i.e., AB_9 and both coloured parts of STAR) have high CuO contents (2.5–3.2 wt%) and negligible CoO, indicating copper as the only chromophore. On the contrary, the samples with the darker shade of blue (i.e., AB_2, BB and Vf) contain both CoO (0.1–0.2 wt%) and CuO, although at lower contents (<1 wt%), hence suggesting the use of cobalt-copper mineralisation in agreement with the evidence from p-XRF (Section 4.1.1) and FORS (4.1.2.). Among these Co-Cu coloured samples, CuO is also present in the white decoration of the LMHK barrel bead (0.17 wt%), whilst it is virtually absent on the white decoration of the Vf natron sample.

NiO is present in significant concentrations (0.31–0.37 wt%) only in the LMHK, darker blue, CoO rich samples (i.e., AB_2, and the blue portion of BB), whilst is absent or negligible (<0.01 wt%) in all the other samples, including the natron one. This suggests that the source of Ni might be the same one as that of Co. A possible explanation for the combined presence of Co and Ni is the use of skutterudite [(Co, Ni, Fe) As₃] that was proposed by Towle et al. (2001) as a source of Co and Cu for the production of European dark blue glasses during the Final Bronze Age. This hypothesis is also supported by the presence of As-rich inclusions detected via SEM-EDS in both samples.

Henderson (1985) suggests, however, that Co could have been obtained as a by-product of the processing of copper or by the use of Cu-Co oxides (e.g., trianite). This could be the case for the natron glass vessel fragment, that presents high CoO and CuO, but not NiO (Table 2), nor As-rich inclusions (Section 4.2.1). The natron sample further differentiates from all the others by being the only one with significant amount of lead, especially in the blue body portion (PbO = 0.2 wt%). Biek and Bayley (1979) suggest that, in the Iron Age, Pb was added to glass artefacts to increase the fluidity of the melt or to increase brilliance, thus explaining its presence in the blue glass batch. It is therefore possible that its presence is not linked to the source of Co and Cu. Interestingly, Vf sample contains also a significant amount of Sb₂O₅, in particular in the opaque white decoration (7.55 wt%): the presence of high quantities of Sb together with high levels of Ca can be linked to the formation of Ca-antimonates, found also by XRD (Section 4.1.3), which produce a white colour as well as opacity (Shortland, 2002). In this context, we can also explain the stark difference in Sb concentration between the white decoration and the blue body (0.9 wt%): in the former, Sb was used to

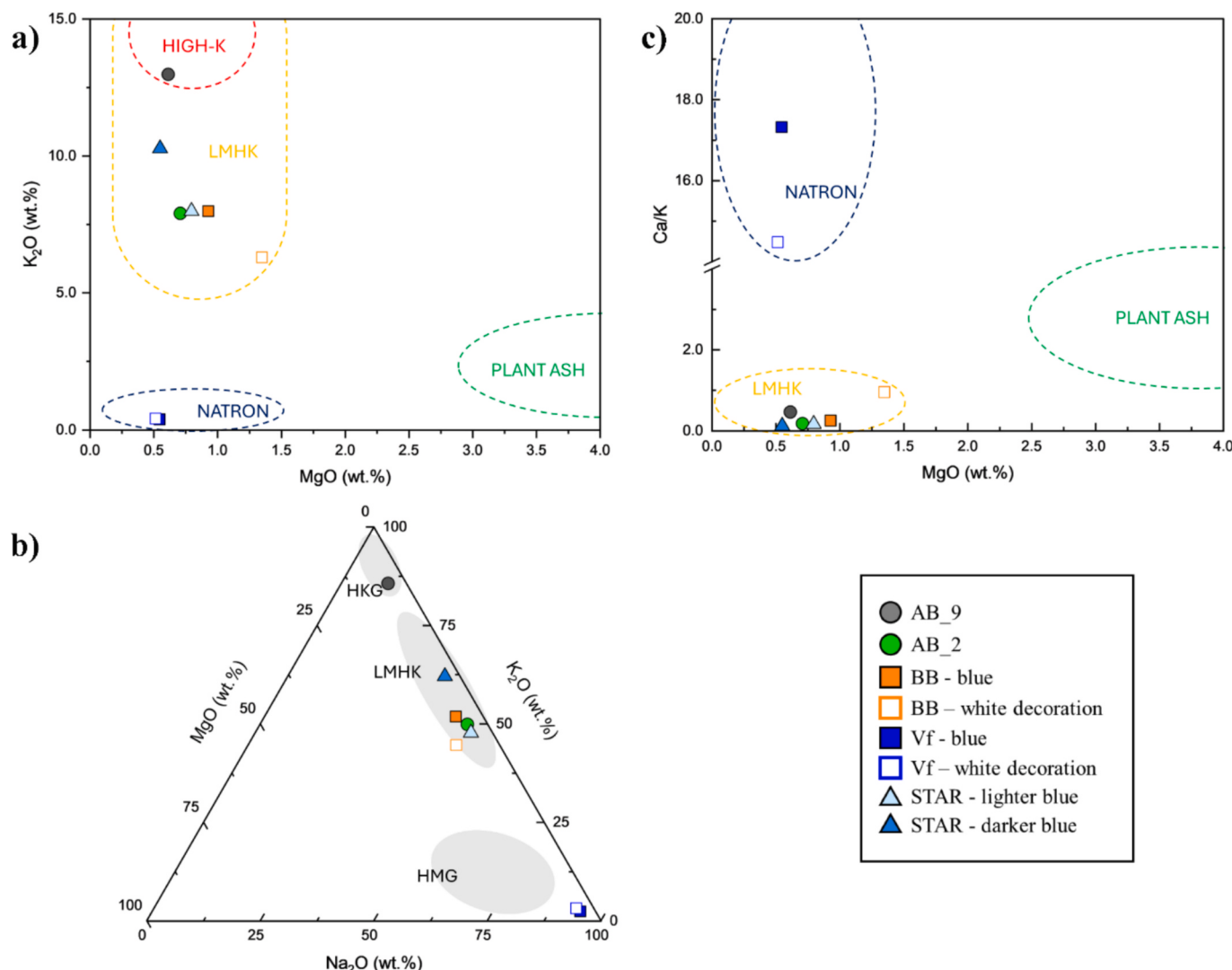


Fig. 7. a) Plot of K_2O vs MgO . Classification on the basis of fluxing agent: compositional fields of natron, LMHK and plant ash glasses (Sayre and Smith, 1961; Henderson, 1988, 1989); b) MgO - Na_2O - K_2O plot and fields defined from grey oval by data of Mildner et al. (2014, 2015), Angelini et al. (2004), Towle et al. (2001) and Venclova et al. (2011), where the HKG represents the field of samples mentioned HIGH-K in this work; c) Plot of Ca/K ratio vs MgO confirms the classification in a).

impart both the opacity and the white coloration, whilst in the latter, a minor amount of Sb was added probably with the sole role of opacifying the glass. In this case, antimony seems to be disconnected from the source of other chromophores.

Lower amounts of Sb_2O_5 , were also found in the BB, but here they increase from the white decoration (0.33 wt%) to the blue body (0.75 wt%). In this case, Sb is associated also with relatively high CuO contents, especially in the blue body ($CuO = 0.97$ wt%), that can be tentatively be explained with the use, for this sample, of tetrahedrite ($(Cu, Fe)_{12}Sb_4S_{13}$), which has been reported for glass productions dated back to the 15th century BCE (e.g., Degryse et al., 2020).

4.2.2.6. Inferences on possible samples provenance. As previously stated (Section 1), the glass compositions can be linked to glass-making recipes typical of specific areas of the Mediterranean and time periods. LMHK glass is commonly associated with Recent and Final Bronze Age Europe (e.g., Frattesina; e.g., Brill, 1992; Angelini et al., 2004), whilst natron glass was commonly produced in the eastern Mediterranean after the I millennium B.C. (e.g., Schlick-Nolte & Werthmann, 2003; Shortland et al., 2006).

Our LMHK and HIGH-K glasses show several characteristics similar

to those ascribed to the Northern Italian production. Their aluminium content is also comparable to that of Frattesina samples (ranging from 1.5 wt% to 2.84 wt%; e.g., Brill, 1992; Angelini et al., 2004; Towle and Henderson, 2004; Conte et al., 2019). The chromophore elements are also compatible with a Northern Italy origin.

The use of Cu alone for light blue samples, and of Co-Cu (plus Ni) for darker blue samples have been reported by Brill (1992) and Conte et al. (2019) for LMHK glasses found directly in the archaeological site of Frattesina, or in glasses from Southern Italy, but still ascribed to the Po valley glass-production. We explained the high Ni and Co (and the presence of As) of the LMHK dark blue coloured sample with a potential of skutterudite (e.g., Towle et al., 2001; Henderson, 2013).

On the contrary, the natron vessel sample shares several features with that produced in South-Eastern Mediterranean centres. The origin of the mineral soda used as fluxing agent is normally liked to Egyptian evaporitic deposits (Turner, 1956; Henderson, 2000; Shortland et al., 2006; Purowski et al., 2012), but natron glass production was widespread also in all the Levant and eastern Mediterranean regions. Indeed, some of the samples found in Southern Italy, dated as early Iron Age, present the same fluxing agent and were linked to the Egyptian production (e.g., Conte et al., 2016, 2019). The use of Ca-antimonates has

also been reported for Egyptian glass (Shortland, 2002).

5. Conclusions

We performed a multi-analytical study, combining the use of non-invasive and non-destructive methods with micro-destructive techniques, on Middle Bronze Age to the Early Iron Age glassy materials from the lakeshore settlement of Paduli (Colli sul Velino, Rieti). This study, presents the first textural, mineralogical and chemical characterization of glass artifacts from Central Italy, providing the opportunity of investigating their glass-making recipes and eventually to attempt tracing their origin hence constraining the trace routes of these object in that period. Thanks to the non-invasive and non-destructive techniques, it was possible to obtain several information about all the analysed samples, considerably reducing the number of the artefacts to be investigated by micro-destructive ones.

The combination of non-invasive and non-destructive with micro-destructive techniques allowed to identify two main glass types. The majority of the samples display the chemical composition of LMHK glass (one of which High-K) with several characteristics comparable to those of glasses from Northern Italian production centres. EMPA data indicate a mixed alkali fluxing agent, likely produced by leaching of plant ashes, which possibly added also CaO as glass stabilizer, consistent also with low Ca/K detected by p-XRF. Non-destructive (i.e. p-XRF and FORS) and EMPA analyses highlight the presence of two main types of chromophores; i) one group of glasses displays a lighter blue/turquoise colour and are characterised by extremely high Cu contents, sometimes associated with sulphur (detected by SEM-EDS), but with negligible amounts of Co, ii) the other group displays a darker blue colour and a chemical composition characterised by significant amounts of both Co, Cu, Ni and in one case Sb, as well as As-rich inclusions (detected by SEM-EDS). The Co-Cu coloured samples can be tentatively related to the use of specific minerals such as skutterudite (rich in Co, Ni and As) or tetrahedrite (rich in Sb).

One sample, Vf, displays, instead, a composition typical of natron glasses, with similarities to glass artifacts produced in the Eastern Mediterranean and Egypt. EMPA data indicate the use of natron as fluxing agent, and the addition of high CaO material as stabilizer, either by the use of an extremely carbonate-enriched silica source or by addition of a specific source of carbonates. The nature of the fluxing agent is confirmed also by the extremely high Ca/K ratio (<14) determined by p-XRF. This glass recipe was typically used in South Mediterranean productions at the beginning of the I millennium B.C (Schlick-Nolte & Werthmann, 2003; Shortland et al., 2006), pointing towards a non-European origin for this glass. The sample displays a dark blue colour achieved by the use of both Co and Cu. Contrary to the LMHK dark blue Co-Cu rich samples, this natron vessel fragment does not present Ni or As, or any other element that can be linked to a specific chromophore-bearing mineral. Such a composition could be explained by the use of Co obtained as a byproduct of Cu-processing using minerals such as trianite ($2\text{CoO}_2\text{-CuO}\cdot6\text{H}_2\text{O}$) (Henderson, 1985). EMPA and p-XRF analyses identified the presence of significant amount of Sb, especially in the white decorations (EMPA), which is confirmed by the occurrence of calcium antimonate detected by XRD. These dispersed particles are responsible for the both the white colour and the opacity of the glass. Minor amount of Sb, determining only the opacity, were also measured in the blue body.

The findings of this work confirm the importance of the Paduli archaeological site in Central Italy at the end of the II millennium BC and its connection with the post-Myceans new trade networks, as also testified by the local metal hoards (Licordari and Virili, 2021).

Our study represents a first step in the characterisation and interpretation of these artifacts that need to be confirmed and integrated by further studies to better constrain the origin of the raw material and the technologies used for their production, as it has been done for glass material from archaeological sites of northern (e.g., Angelini et al.,

2004; Henderson et al., 2015) and the southern Italy (e.g., Conte et al., 2016; 2019).

Glassy materials retain the same major characteristics for long periods of time and for different provenances (Tanimoto & Rehren, 2008), making it necessary to use multiple parameters to determine the provenance and to correctly ascertain their origin and the raw materials used for their production. Therefore, these results need to be corroborated by further geochemical investigation, such as trace elements, REE (Rare Earth Elements) contents (e.g., Shortland et al., 2007) and isotopic fingerprints of specific elements (e.g., Sr and Nd; Henderson et al., 2015, Blomme et al., 2017; Conte et al., 2018), which could be used also for interesting and more in-depth comparison with existing literature data on glass samples coming from major glass-production centres active during the Final Bronze Age – Early Iron Age period. These analyses are currently in progress and will be published in due course.

Useful information might also come from more powerful analytical techniques such as X-ray absorption spectroscopy (XAS), fundamental to understand the colouring/decolouring mechanisms of the chromophore ions and the structural role of the chemical species in the glass (Angelini et al., 2019), which in turn might lead to more insight into the process used for the realization of these glassy materials and on the technology available at the time.

CRediT authorship contribution statement

Silvia Vettori: Writing – review & editing, Writing – original draft, Visualization, Validation, Supervision, Methodology, Investigation, Conceptualization. **Francesca Giannetti:** Writing – review & editing, Writing – original draft, Visualization, Validation, Investigation. **Eleonora Braschi:** Writing – review & editing, Writing – original draft, Visualization, Methodology, Investigation. **Riccardo Avanzinelli:** Writing – review & editing, Writing – original draft, Visualization, Investigation, Conceptualization. **Carlo Virili:** Writing – original draft, Resources, Conceptualization. **Alessandro M. Jaia:** Resources, Funding acquisition. **Alessandro Zanini:** Writing – review & editing, Writing – original draft, Resources, Conceptualization. **Emma Cantisani:** Writing – review & editing, Writing – original draft, Visualization, Validation, Methodology, Investigation, Conceptualization.

Acknowledgments

The authors wish to thank to Dr. Giovanni Bartolozzi of the CNR-IFAC for granting the access to the FORS instrumentation and his support during the measurements. The authors are also thankful to Dr. Laura Chelazzi (at CRIST, Centro di Servizi di Cristallografia Strutturale of the University of Florence), Dr. Laura Chiarantini (MEMA, Centro di Servizi di Microscopia Elettronica e Microanalisi of the University of Florence) and Dr. Jacopo Orsilli (Department of Materials Science, University of Milano-Bicocca) for the patience and precious support.

Appendix A. Supplementary data

Supplementary data to this article can be found online at <https://doi.org/10.1016/j.jasrep.2025.105396>.

Data availability

Data will be made available on request.

References

- Angelini, I., 2011. Archaeometry of Bronze Age and Early Iron Age Italian Vitreous Materials: A Review, in: Turbanti-Memmi, I., (Eds), Proceedings of the 37th International Symposium on Archaeometry, 13th - 16th May 2008, Siena, Italy. Springer, Berlin, Heidelberg. Doi: 10.1007/978-3-642-14678-7_3.

- Angelini, I., Artioli, G., Bellintani, P., Diella, V., Gemmi, M., Polla, A., Rossi, A., 2004. Chemical analyses of Bronze Age glasses from Frattesina di Rovigo, northern Italy. *J. Archaeol. Sci.* 31 (8), 1175–1184. <https://doi.org/10.1016/j.jas.2004.02.015>.
- Angelini, I., Artioli, G., Bellintani, P., Diella, V., Polla, A., Recchia, G., Residori, G., 2003. Materiali vetrosi da Grotta Manaccora e Coppa Nevigata: inquadramento archeologico e archeometrico nell'ambito della civiltà del bronzo italiana, in: Piccioli, C., Sogliani, F. (Eds.), Il vetro in Italia meridionale e insulare. Atti del secondo congresso multidisciplinare, pp. 127–138.
- Angelini, I., Artioli, G., Bellintani, P., Diella, V., Polla, A., Residori, G., 2002. Project Glass materials in the Protohistory of North Italy, a first summary. In: d'Amico, C. (Ed.), Atti Del Secondo Congresso Nazionale Di Archeometria. Patron Editore, Bologna, Italy, pp. 581–595.
- Angelini, I., Artioli, G., Bellintani, P., Polla, A., 2005. Protohistoric vitreous materials of Italy: from Early faience to Final Bronze Age glasses, in: AIHV, Annales du 16 Congrès de l'Association Internationale pour l'Histoire du Verre, 32–36.
- Angelini, I., Artioli, G., Polla, A., de Marinis, R., 2006. Early Bronze age faience from north Italy and Slovakia: a comparative archaeometric study, in: Proceeding of the 34th symposium of Archeaometry, Zaragoza Spain, 2006, 371–378.
- Angelini, I., Gratuze, B., Artioli, G., 2019. Glass and other vitreous materials through history, in: Artioli, G., Oberri, R., The Contribution of Mineralogy to Cultural Heritage. Doi: 10.1180/EMU-notes.20.3.
- Arletti, R., Bertoni, E., Vezzalini, G., Mengoli, D., 2011. Glass beads from Villanovan excavation in Bologna (Italy): an archaeometrical investigation. *Eur. J. Mineral.* 23, 959968. <https://doi.org/10.1127/0935-1221/2011/0023-2166>.
- Arletti, R., Ciarralo, A., Quartieri, S., Sabatino, G., Vezzalini, G., 2006a. Archaeometrical analyses of Game counters from Pompeii. In: Maggetti, M., Messiga, B. (Eds.), Geomaterial in Cultural Heritage, Special Publication, vol. 257. Geological Society of London, London, pp. 175–186. <https://doi.org/10.1144/GSL.SP.2006.257.01.14>.
- Arletti, R., Quartieri, S., Vezzalini, G., 2006b. Glass mosaic tesserae from Pompeii: an archaeometrical investigation. *Periodico Mineralogia* 76, 25–38.
- Artioli, G., Angelini, I., Polla, A., 2008. Crystals and phase transitions in protohistoric glass materials. *Phase Transit.* 81 (2–3), 233–252. <https://doi.org/10.1080/01411590701514409>.
- Barkoudah, Y., Henderson, J., 2006. Plant ashes from Syria and the manufacture of ancient glass: ethnographic and scientific aspects. *J. Glass Stud.* 297–321.
- Bellintani, P., 2011. Progetto "Materiali vetrosi della protostoria italiana". Aggiornamenti e stato della ricerca. *Rivista Di Scienze Preistoriche* 66, 257–282.
- Bellintani, P., 2014. Baltic amber, alpine copper and glass beads from the Po plain. Amber trade at the time of Campestrin and Frattesina. *Padvs* 50, 111–139.
- Bellintani, P., Saracino, M., 2015. Rivers, human occupation and exchanges around the late Bronze Age settlement of Frattesina (ne Italy). In: Vianello, A. (Ed.), *Rivers in Prehistory*. Oxford, pp. 77–87.
- Bellintani, P., Angelini, I., 2020. I vetri di Frattesina. Caratterizzazione crono-tipologica, archeometria e confronti nell'ambito della tarda età del Bronzo dell'Europa centro-orientale e del Mediterraneo, in: Frattesina cinquant'anni dopo. Il Delta del Po tra Europa e Mediterraneo nei secoli attorno al 1000 aC. Padusa, 56 (Tomo I), 71–118.
- Biavati, A., Verità, M., 1989. The glass from Frattesina, a glassmaking center in the late Bronze Age. *Rivista Della Stazione Sperimentale Del Vetro* 4, 295–299.
- Biek, L., Bayley, J., 1979. Glass and other vitreous materials. *World Archaeol.* 11 (1), 1–25. <https://doi.org/10.1080/00438243.1979.9979746>.
- Bonizzoni, L., Galli, A., Gondola, M., Martini, M., 2013. Comparison between XRF, TXRF, and PXRF analyses for provenance classification of archaeological bricks. *X-Ray Spectrom.* 42, 262–267. <https://doi.org/10.1002/xrs.2465>.
- Brill, R.H., 1992. Chemical analyses of some glasses from Frattesina. *J. Glass Stud.* 34, 11–22.
- Butler, K.H., Bergin, M.J., Hannaford, V.M.B., 1950. Calcium Antimonates. *J. Electrochem. Soc.* 97 (4), 117–122.
- Conte, S., Arletti, R., Henderson, J., Degryse, P., Blomme, A., 2018. Different glassmaking technologies in the production of Iron Age black glass from Italy and Slovakia. *Archaeol. Anthropol. Sci.* 10, 503–521. <https://doi.org/10.1007/s12520-016-0366-4>.
- Conte, S., Arletti, R., Mermati, F., Gratuze, B., 2016. Unravelling the Iron Age glass trade in southern Italy: the first trace-element analyses. *Eur. J. Mineral.* 28 (2), 409–433. <https://doi.org/10.1127/ejm/2016/0028-2516>.
- Conte, S., Matarese, I., Quartieri, S., Arletti, R., Jung, R., Pacciarelli, M., Gratuze, B., 2015. Bronze Age vitreous materials from Punta di Zambrone (southern Italy). *Eur. J. Mineral.* 27 (3), 337–351. <https://doi.org/10.1127/ejm/2015/0027-2450>.
- Conte, S., Matarese, I., Vezzalini, G., Pacciarelli, M., Scarano, T., Vanzetti, A., Gratuze, B., Arletti, R., 2019. How much is known about glassy materials in Bronze and Iron Age Italy? New data and general overview. *Archaeol. Anthropol. Sci.* 11 (5), 1813–1841. <https://doi.org/10.1007/s12520-018-0634-6>.
- Curci, A., Fiori, F., Cavazzuti, C., D'Auria, A., Vanacore, L., Virili, C., Jaia, A.M., forthcoming. Il contributo delle bioarcheologie nel progetto di ricerca del sito di Paduli (Colli sul Velino, RI): economia ed ambiente tra la fine del Bronzo finale e gli inizi dell'età del Ferro, in: Atti IIPP LXVI.
- Dardeniz, G., 2015. Was ancient Egypt the only supplier of natron?: New research reveals major anatolian deposits. *Anatolica* 41, 191–202. <https://doi.org/10.2143/ANA.41.0.3127293>.
- Dardeniz, G., Henderson, J., Roe, M., 2022. Primary evidence for glassmaking in late Bronze Age Alalah/Tell Atchana (Amaq Valley, Turkey). *J. of Glass Stud.* 64, 11–32.
- Degryse, P., Shortland, A.J., 2020. Interpreting elements and isotopes in glass: a review. *Archaeometry* 62, 117–133. <https://doi.org/10.1111/arcm.12531>.
- Degryse, P., Shortland, A.J., Dillis, S., van Ham-Meert, A., Vanhaecke, F., Leeming, P., 2020. Isotopic evidence for the use of Caucasian antimony in late Bronze Age glass making. *J. Archaeol. Sci.* 120, 105195. <https://doi.org/10.1016/j.jas.2020.105195>.
- Diamond, J., 2007. Collasso: come le società scelgono di morire o vivere. Einaudi editore, Torino.
- Fermo, P., Andreoli, M., Bonizzoni, L., Fantauzzi, M., Giubertoni, G., Ludwig, N., Rossi, A., 2016. Characterisation of Roman and byzantine glasses from the surroundings of Thugga (Tunisia): Raw materials and colours. *Microchem. J.* 129, 5–15. <https://doi.org/10.1016/j.microc.2016.05.014>.
- Freestone, I.C., 2006. Glass production in late Antiquity and the Early Islamic period: a geochemical perspective. *Geol. Soc. Lond. Spec. Publ.* 257 (1), 201–216. <https://doi.org/10.1144/GSL.SP.2006.257.01.16>.
- Freestone, I.C., Leslie, K.A., Thirlwall, M., Gorin-Rosen, Y., 2003. Strontium isotopes in the investigation of early glass production: byzantine and early Islamic glass from the Near East. *Archaeometry* 45, 19–32. <https://doi.org/10.1111/1475-4754.00094>.
- Gallo, F., Silvestri, A., Molin, G., 2013. Glass from the archaeological Museum of Adria (north-east Italy): new insights into early roman production technologies. *J. Archaeol. Sci.* 40 (2013), 2589–2605. <https://doi.org/10.1016/j.jas.2013.01.017>.
- Gliozzo, E., 2017. The composition of colourless glass: a review. *Archaeol. Anthropol. Sci.* 9, 455–483. <https://doi.org/10.1007/s12520-016-0388-y>.
- Gliozzo, E., Barbone, A.S., D'acapito, F., 2013. Waste glass, vessels and window-panes from Thamusida (morocco): grouping natron-based blue-green and colourless Roman glasses. *Archaeometry* 55, 609–639. <https://doi.org/10.1111/j.1475-4754.2012.00696.x>.
- Hartmann, G., Kappel, I., Grote, K., Arndt, B., 1997. Chemistry and technology of prehistoric glass from Lower Saxony and Hesse. *J. Archaeol. Sci.* 24 (6), 547–559. <https://doi.org/10.1006/jasc.1996.0138>.
- Henderson, J., 1985. The raw materials of early glass production. *Oxford J. Archaeol.* 4 (3), 267–291. <https://doi.org/10.1111/j.1468-0092.1985.tb00248.x>.
- Henderson, J., 1988. Electron probe microanalysis of mixed-alkali glasses. *Archaeometry* 30 (1), 77–91. <https://doi.org/10.1111/j.1475-4754.1988.tb00436.x>.
- Henderson, J., 1989. The scientific analysis of ancient glass and its archaeological interpretation, in: Scientific analysis in archaeology and its interpretation. Oxford University Committee for Archaeology, Monograph, 19, 30–62.
- Henderson, J., 2000. The science and Archaeology of materials: an investigation of inorganic materials. Ed. Routledge, London. Doi: 10.4324/9780203630143.
- Henderson, J., 2013. *Ancient glass, an interdisciplinary exploration*. Cambridge University Press, New York.
- Henderson, J., Evans, J., Bellintani, P., Bietti-Sestieri, A.M., 2015. Production, mixing and provenance of late Bronze Age mixed alkali glasses from northern Italy: an isotopic approach. *J. Archaeol. Sci.* 55, 1–8. <https://doi.org/10.1016/j.jas.2014.12.000>.
- Henderson, J., Evans, J.A., Sloane, H.J., Leng, M.J., Doherty, C., 2005. The use of oxygen, strontium and lead isotopes to provenance ancient glasses in the Middle East. *J. Archaeol. Sci.* 32 (5), 665–673. <https://doi.org/10.1016/j.jas.2004.05.008>.
- Henderson, J., McLoughlin, S.D., McPhail, D.S., 2004. Radical changes in Islamic glass technology: evidence for conservatism and experimentation with new glass recipes from early and middle Islamic Raqqa, Syria. *Archaeometry* 46 (3), 439–468. <https://doi.org/10.1111/j.1475-4754.2004.00167.x>.
- Jaja, A.M., Virili, C., Curci, A., Fiori, F., Di Pasquale, G., D'Auria, A., 2020. Il sito periacastre di epoca protostorica di loc. Paduli (Colli sul Velino, RI). Indagini di superficie 2011–2013 e saggio di scavo 2015. *Preistoria e Protostoria in Etruria*, 1, 415–444.
- Jennings, B., 2014. Travelling objects: changing values: the role of northern Alpine lake-dwelling communities in exchange and communication networks during the late Bronze Age. Archaeopress Publishing Ltd.
- Lahlil, S., Biron, I., Galoisy, L., Morin, G., 2008. Rediscovering ancient glass technologies through the examination of opacifier crystals. *Appl. Phys. A* 92, 109–116. <https://doi.org/10.1007/s00339-008-4456-8>.
- Lahlil, S., Biron, I., Cotte, M., Susini, J., Mengury, N., 2010. Synthesis of calcium antimonate nano-crystals by the 18th dynasty Egyptian glassmakers. *Appl. Phys. A* 98, 1–8. <https://doi.org/10.1007/s00339-009-5454-1>.
- Licordari, F., Virili, C., 2021. I paesaggi d'acqua di Colli sul Velino, in: Landscapes. Paesaggi culturali, maggio 2019, Roma, Atti della Giornata di Studi, Roma: Fondazione Dià Cultura, 71–87.
- Lilyquist, C., Brill, R.H., Wypyski, M.T., 1993. *Studies in early Egyptian glass*. Metropolitan Museum of Art.
- Meulebroeck, W., Baert, K., Wouters, H., Cosyns, P., Ceglia, A., Cagno, S., Janssens, K., Nys, K., Terrey, H., Thienpont, H., 2010. The identification of chromophores in ancient glass by the use of UV-VIS-NIR spectroscopy. *Proc. SPIE* 7726, Optical Sensing and Detection, 77260D (13 May 2010). Doi: 10.1117/12.853666.
- Meulebroeck, W., Wouters, H., Nys, K., Thienpont, H., 2016. Authenticity screening of stained glass windows using optical spectroscopy. *Sci. Rep.-UK* 6 (1), 37726. <https://doi.org/10.1038/srep37726>.
- Micheletti, F., Orsilli, J., Melada, J., Gargano, M., Ludwig, N., Bonizzoni, L., 2020. The role of IRT in the archaeometric study of ancient glass through XRF and FORS. *Microchem. J.* 153, 104388. <https://doi.org/10.1016/j.microc.2019.104388>.
- Mildner, S., Schuessler, U., Falkenstein, F., Brätz, H., 2014. Bronzezeitliches Glas im westlichen Mitteleuropa – Funde, Zusammensetzung und die Frage nach seiner Herkunft, in: Nessel, B., Heske, I., Brandherm, D. (Eds.), Ressourcen und Rohstoffe in der Bronzezeit. Nutzung – Distribution – Kontrolle. Arbeitsberichte zur Bodendenkmalfpflege in Brandenburg 26 (Zossen 2014), pp. 100–108.
- Mildner, S., Schuessler, U., Falkenstein, F., Brätz, H., 2015. Mitteleuropäisches "High-Magnesium-Glass" – Erste Ergebnisse einer archäometrischen Untersuchung zu bronzezeitlichen Glasperlen, in: Gluhak, T., Greiff, S., Kraus, K., Prange, M. (Eds.), Metalla, Sonderheft 7, Archäometrie und Denkmalpflege 2015, Jahrestagung an der Johannes-Gutenberg-Universität Mainz, 25–28 März 2015, pp. 81–83.

- Mirti, P., Lepora, A., Saguì, L., 2000. Scientific analysis of seventh-century glass fragments from the Crypta Balbi in Rome. *Archaeometry* 42, 359–374. <https://doi.org/10.1111/j.1475-4754.2000.tb00887.x>.
- Möncke, D., Papageorgiou, M., Winterstein-Beckmann, A., Zacharias, N., 2014. Roman glasses coloured by dissolved transition metal ions: redox-reactions, optical spectroscopy and ligand field theory. *J. Archaeol. Sci.* 46, 23–36. <https://doi.org/10.1016/j.jas.2014.03.007>.
- Moorey, P.R.S., 1985. Materials and Manufacture in Ancient Mesopotamia: The Evidence of Archaeology and Art. Oxford: British Archaeological Reports, BAR publishing, International Series 237, pp. 330.
- Nicholson, P.T., 1993. Egyptian Faience and Glass, No. 18. Shire Publications.
- Oppenheim, A.L., 1973. Towards a history of glass in the ancient Near East. *J. Am. Oriental Soc.* 259–266.
- Pouchou, J.L., Pichoir, F., 1991. Quantitative Analysis of Homogeneous or Stratified Microvolumes Applying the Model "PAP", in: Heinrich, K.F.J. and Newbury, D.E., Eds., Electron Probe Quantification, Plenum Press, New York, 31–75. Doi: 10.1007/978-1-4899-2617-3_4.
- Purowski, T., Dzierżanowski, P., Bulska, E., Wagner, B., Nowak, A., 2012. A study of glass beads from the Hallstatt C-D from South-Western Poland: implications for glass technology and provenance. *Archaeometry* 54 (1), 144–166. <https://doi.org/10.1111/j.1475-4754.2011.00619>.
- Purowski, T., Kępa, L., Wagner, B., 2018. Glass on the Amber Road: the chemical composition of glass beads from the Bronze Age in Poland. *Archaeol. Anthropol. Sci.* 10, 1283–1302.
- Santopadre, P., Verità, M., 2000. Analyses of the production technologies of Italian vitreous materials of the Bronze Age. *J. Glass Stud.* 42, 25–40.
- Sayre, E.V., Smith, R.W., 1961. Compositional categories of ancient glass. *Science* 133 (3467), 1824–1826. <https://doi.org/10.1126/science.133.3467.1824>.
- Schlick-Nolte, B., Werthmann, R., 2003. Glass vessels from the burial of Nesikhons. *J. Glass Stud.* 11–34.
- Shortland, A.J., 2000. Vitreous materials at Amarna: the production of glass and faience in 18th Dynasty Egypt. BAR Publishing. <https://doi.org/10.30861/9781841710389>.
- Shortland, A.J., 2002. The use of antimonate colorants in Early Egyptian Glass. *Archaeometry* 44, 517–530. <https://doi.org/10.1111/1475-4754.t01-1-00083>.
- Shortland, A.J., Eremin, K., 2006. The analysis of second millennium glass from Egypt and Mesopotamia: part 1: new WDS analyses. *Archaeometry* 48 (4), 581–603. <https://doi.org/10.1111/j.1475-4754.2006.00274.x>.
- Shortland, A., Rogers, N., Eremin, K., 2007. Trace element discriminants between Egyptian and Mesopotamian late Bronze Age glasses. *J. Archaeol. Sci.* 34 (5), 781–789. <https://doi.org/10.1111/j.1475-4754.2006.00274.x>.
- Shortland, A., Schachner, L., Freestone, I., Tite, M., 2006. Natron as a flux in the early vitreous materials industry: sources, beginnings and reasons for decline. *J. Archaeol. Sci.* 33 (4), 521–530. <https://doi.org/10.1016/j.jas.2005.09.011>.
- Stevens, S.J., Hand, R.J., Sharp, J.H., 1997. Polymorphism of silica. *J. of Mater. Sci.* 32, 2929–2935. <https://doi.org/10.1023/A:1018636920023>.
- Towle, A., Henderson, J., 2004. The glass bead game: archaeometric evidence for the existence of an Etruscan glass industry. *Etruscan Studies* 10 (1), 47–66. <https://doi.org/10.1515/est.2004.10.1.47>.
- Towle, A., Henderson, J., Bellintani, P., Gambacurta, G., 2001. Frattesina and Adria: report of scientific analyses of early glass from the Veneto. *Padusa* 37, 7–68.
- Turner, W., 1954. Studies of ancient glasses and glassmaking processes. Part i. *J. Soc. Glass Technol.* 38, 436–444.
- Turner, W.E.S., 1956. Studies of ancient glass and glassmaking processes. Part V: Raw materials and melting processes. *J. Soc. Glas. Technol.* 40, 277–300. <https://doi.org/10.1039/PS9610000093>.
- Van der Linden, V., Meesdom, E., Devos, A., Van Dooren, R., Niejdorp, H., Janssen, E., Balace, S., Vekemans, B., Vincze, L., Janssens, K., 2011. PXRF, μ -XRF, vacuum μ -XRF, and EPMA analysis of email Champlévé objects present in Belgian museums. *Microsc. Microanal.* 17, 674–685. <https://doi.org/10.1017/S1431927611011950>.
- Venclová, N., Huřinský, V., Henderson, J., Chenery, S., Šulová, L., Hložek, J., 2011. Late Bronze Age mixed-alkali glasses from Bohemia. *Archeol. Rozhl.* 63, 559–585.
- Virili, C., 2021. La Piana di Rieti ed il bacino di Piediluco tra Bronzo Antico e Bronzo Medio: un lungo processo verso le prime forme di popolamento stabile e capillare del territorio. In: Betori, A., Licordari, F., Piermattei, P. (Eds.), Lungo Il Corso Del Velino. Roma, Officina Edizioni, pp. 179–226.
- Virili, C., 2022. Paesaggi d'acqua velini: il sito perilastrone di località Paduli. In: Virili, C. (Ed.), Rieti Città Delle Acque. Studi e Ricerche Di Geologia, Archeologia e Storia Dell'agro Reatino. Teseo Editore, Rieti, pp. 121–154.
- Virili, C., Jaia, A.M., Zanini, A., Cantisani, E., Vettori, S., Vanacore, L., D'Auria, A., 2022. Il sito perilastrone di epoca protostorica di loc. Paduli (Colli sul Velino, RI). Indagini radiometriche, archeometriche e paleobotaniche, Atti PPE XIV, 779–813.
- Wedepohl, K.H., Baumann, A., 2000. The use of marine molluskan shells for Roman glass and local raw glass production in the Eifel area (Western Germany). *Naturwissenschaften* 87, 129–132. <https://doi.org/10.1007/s00140050690>.
- Yatsuk, O., Koch, L., Gorghinian, A., Fiocco, G., Davit, P., Giannossa, L.C., Mangone, A., Francone, S., Serges, A., Re, A., Lo Giudice, A., Ferretti, M., Malagodi, M., Iaia, C., Gulmini, M., 2023. An archaeometric contribution to the interpretation of blue-green glass beads from Iron age Central Italy. *Heritage Sci.* 11, 113. <https://doi.org/10.1186/s40494-023-00952-1>.